modification of diet in renal disease equation in the japanese general population Iwate KENCO Study.
Circulation Journal 77(5): 1315-1325, 2013.

Saito H, Ogasawara K, Nishimoto H, Yoshioka Y, Murakami T, Fujiwara S, Sasaki M, Kobayashi M, Yoshida K, Kubo Y, Beppu T, Ogawa A.
Postoperative changes in cerebral metabolites associated with cognitive improvement and impairment after carotid endarterectomy: a 3T proton MR spectroscopy study.
American journal of Neuroradiology 34(5): 976-982, 2013.

Takahashi Y, Ogasawara K, Matumoto Y, Kobayashi M, Yoshida K, Kubo Y, Beppu T, Murakami T, Nanba T, Ogawa A.
Changes in cognitive function after carotid endarterectomy in older patients: comparison with younger patients.
Neurologia medico-chirurgica 53(6): 353-359, 2013.

Matsumoto Y, Ogasawara K, Saito H, Terasaki K, Takahashi Y, Ogasawara Y, Kobayashi M, Yoshida K, Beppu T, Kubo Y, Fujiwara S, Tsushima E, Ogawa A.
Detection of misery perfusion in the cerebral hemisphere with chronic unilateral major cerebral artery steno-occlusive disease using crossed cerebellar hypoperfusion: comparison of brain SPECT and PET imaging.
European Journal of Nuclear Medicine and Molecular Imaging 40(10): 1573-1581, 2013.

Oikawa K, Ogasawara K, Saito H, Yoshida Koji, Saura H, Sato Y, Terasaki K, Wada T, Kubo Y.
Combined measurement of cerebral and cerebellar blood flow on preoperative brain perfusion SPECT imaging predicts development of new cerebral ischemic events after endarterectomy for symptomatic unilateral cervical carotid stenosis.
Clinical Nuclear Medicine 38(12): 957-961, 2013.

Sato Yuiko, Ito K, Ogasawara K, Sasaki M, Kudo K, Murakami T, Nanba T, Nishimoto H, Yoshida K, Kobayashi M, Kubo Y, Mase T, Ogawa A.
Postoperative increase in cerebral white matter fractional anisotropy on diffusion tensor magnetic resonance imaging is associated with cognitive improvement after uncomplicated carotid endarterectomy: tract-based spatial statistics analysis.
Neurosurgery 73(4): 592-599, 2013.

2. 学会発表
国内学会
小笠原 邦昭
ミニブタおよび疑似血管モデルを用いたCEAの手技トレーニング
第22回脳神経外科手術と機器学会(CNTT) 松本
2013年4月

小笠原　邦昭
TCD モニタリングを用いた頸動脈内膜剥離術中脳合併症の診断と対策
第 32 回日本脳神経超音波学会総会　徳島 2013 年 6 月

小笠原　邦昭
慢性脳虚血性病変に対する血行再建術と頭痛
第 41 回日本頭痛学会総会　盛岡　2013 年 11 月

H. 知的財産権の出願・登録状況
特記事項なし

厚生労働科学研究費補助金(医療機器開発推進研究事業)

分担研究報告書

脳内留置型微細内視鏡の開発と前臨床試験研究 (H23-医療機器-指定-001)

研究分担者　佐藤 洋一　岩手医科大学　解剖学　　教授

ヒトに使用可能な蛍光プローブの開発研究:　血管イメージングと光毒性の基礎的検討

研究要旨

蛍光色素を負荷した血管標本を用いて、立体イメージングを試みた。炎症機転の重要な場である細静脈の血管平滑筋を、細動脈平滑筋と比較して、どのような形態的・能的相違があるかを、光顕・電顕観察ならびにカルシウム感受性蛍光色素を用いて検討を加えた。脳循環のイメージングに先立ち、精巣の血管系で解析を始めた。その結果、細動脈平滑筋は紡錘形をして輪状に配列しているのに対し、細静脈平滑筋は多角形を呈していることがわかった。また、細動脈で強い反応を引き起こすATPやセロトニンでは。細静脈の反応が起きなかったが、ノルアドレナリンやアンギオテンシンで強い反応が生じた。なお、眼球の細静脈ではATPに対する反応が強く見られたことから、脳循環は他の器官におけるものと著しい差があることが示唆されている。

A 研究目的

さまざまな細胞の反応性を調べるために、蛍光色素（物質）を用いた生体イメージングが盛んにおこなわれているが、その多くが培養単離細胞でなされており、生体内で起きている状況を正確にシミュレートしているかどうかはわからない。循環メカニズムに関しては多くの研究が動脈系についてなされているものの静脈系では研究が進んでいない。そこで本分担者は、脳内血管のイメージングに向けた予備実験として、蛍光色素を負荷した細動脈と細静脈のイメージングの可能性を検証することを目的として、反応性の検証をした。平成２４年度報告書にあるように、イメージングによる光毒性は、ほぼ無視できることから、平成２５年度はカルシウムイメージングを中心に以下の実験をおこなった。

B 研究方法

ラット精巣と眼球から細動脈と細静脈を分離し、標本とした。【血管平滑筋の形態観察】細静脈と細動脈標本を常法に従って固定し電子顕微鏡標本と光学顕微鏡標本を作製した。後者は全載標本として、アクチンを蛍光色素標識されたファラシジンで染め出して観察した。【血管平滑筋の反応性解析】カルシウムイオン感受性蛍光色素(Indo-1)を負荷した後、360nmのレーザーを照射して440nmを境として長波長側と短波長側の蛍光を除算して、細胞内カルシウムイオン濃度($[Ca^{2+}]_i$)を反映する蛍光比画像をリアルタイムで取得した。刺激薬として、ノルアドレナリン、セロトニン、ATPとアンギオテンシンを、抑制薬としてサプシガルギンを用いた。

（倫理面への配慮）

岩手医科大学実験動物センターの実験指針に則って、実験を行った。

C 研究結果

【血管平滑筋の形態観察】

細動脈では紡錘形の平滑筋が１～３層輪状に取り巻くのに対し、細静脈では１層の多角形～星形の平滑筋細胞が配列していた。また細静脈の平滑筋細胞は敷石状に並んでいるとは言え、細胞間に隙間が見られた。そこで細胞間の接合を詳細に観察するため、準薄切切片をＳＴＥＭモードで観察して立体構築を試みる実験を始めた。

【細動脈と細静脈の血管平滑筋の反応性の解析】

細動脈は組織内血流制御において、また細静脈は炎症機転の場として重要である。そうした血管本来の組織形態を保ったままの血管標本で$[Ca^{2+}]_i$変動を観察したところ、細動脈の紡錘形をした平滑筋は、ノルアドレナリン、セロトニン、ATP、アンギオテンシンⅡによって$[Ca^{2+}]_i$が上昇したが、細静脈の多角形をした平滑筋はノルアドレナリンとアンギオテンシンに対する反応が見られたものの、セロトニンやATPに対する反応は認められなかった。ノルアドレナリンとアンギオテンシンⅡに対する細静脈平滑筋の反応は、細胞外カルシウムを除去しても観察されたが、サプシガルギン前処理で抑制されたことから、細胞内カルシウム貯蔵場からの動員機転が関与していることが確かめられた。但し、眼球から採取された細静脈の血管平滑筋はATPによって反応が引き起こされた。これがP2X受容体によるものか、P2Y受容体が関与しているものかを明らかにする必要がある。

D 考察

組織本来の形態を保ったままの標本で時系列的に連続したイメージングが可能であることから、in vivoイメージングでカルシウムイメージングをおこなうことができると期待される。そこで実験のターゲットを絞るため、平成２５年度は静脈系と動脈系の平滑筋の反応性をあらかじめ確かめたが、その結果は、血管系の差と部位（臓器）差がかなりあることが示された。

平滑筋細胞の形が異なることから、機能的意義も異なることが容易に想像されるとは言え、いままできちんとした解析がなされてこなかった。今回の結果は、いわいる昇圧物質は静脈平滑筋の反応を引き起こすが、局所的な伝達物質に過ぎないATPやセロトニンは、細静脈の反応を引き起こしていない。則ち、全身的な血圧上昇という現象は細動脈血管抵抗だけではなく静脈系の反応も考慮しなければいけないことを示している。尤も、中枢神経系の静脈は、他の臓器の静脈系と異なっていることが予想されることから、脳表面の細静脈を採取した実験を加えなければならないが、現在、難航している。そこで比較的採取が簡単な眼球の血管系で実験を施行している。

F.　健康危険情報

なし

E 結論

血管平滑筋の多様性に富む反応性の解析には、$[Ca^{2+}]_i$変動を観察できるin vivoの実験系が有用であろう。但し。臓器による差、血管系による差を検証する標本系の作成が前提となると思われた。

G 研究発表

1. 論文発表

なし

2. 学会発表

国際学会

Yoh-ichi Satoh, Tomoyuki Saino, Kazuki Masu, Makoto Matsuura, Toshinari Misaki, Yasunori Tamakawa, Kana Sasaki

Functional heterogeneity of blood vessels: with special reference to Ca2+ dynamics of smooth muscles.

International Symposium Anatomical Science for advance in health and clinical therapy, Aug 2013, Sendai

国内学会

佐々木香奈、平川正人、齋野朝幸、佐藤洋一

血管平滑筋の細胞内カルシウム動態に及ぼす神経伝達物質の効果－細動脈と細静脈の比較－.

第59回日本解剖学会東北・北海道連合支部学術集会　2013年 9月, 札幌

Higashio H, Satoh Y

The GTPase Rab37 participates in the control of mast cell degranulation.

第36回日本分子生物学会年会, 12.3-12.6/ 2013, 神戸

H. 知的財産権の出願・登録状況

特記事項なし

厚生労働科学研究費補助金(医療機器開発推進研究事業)

分担研究報告書

脳内留置型微細内視鏡の開発と前臨床試験研究 (H23-医療機器-指定-001)

研究分担者　平　英一　岩手医科大学　薬理学　　教授

研究要旨

重症頭部外傷や重症くも膜下出血後の頭蓋内環境のモニタリングを持続的に行うことは、その治療において大変重要である。そこで脳内留置型微細内視鏡の開発とインドシアニングリーン (ICG) を用いた脳血管機能解析法開発、その基盤となるICGの脳血管描出能の検討をおこなう事が中心テーマである。本研究においては、血管に対するインドシアニングリーンやその描出に用いる光の血管構成細胞に対する影響を検討することと、内視鏡を留置した際の周囲結合織の形成機構について検討した。

A 研究目的

血管内皮細胞及び、平滑筋細胞は生体内においては常時メカニカルストレスを受けており、培養下においても同様のストレスを与えることは生理的環境に近いと考えられる。今回、蛍光やインドシアニングリーン負荷のこれらの細胞に与える影響を検討するにあたり、今回の実験に用いるストレックスシステムによるメカニカルストレス下での各培養細胞における発現形質の変化を静置培養と比較した。

B 研究方法

メカニカルストレスを与えるためにストレックスシステムを用いた。平滑筋細胞はシリコン性チャンバーをコラーゲン溶液でコーティングして接着させ、血管内皮細胞はコラーゲン上に更にゼラチンコーティングを行って接着させた。この後48時間静置培養し、その後に48時間伸展培養してから細胞を採取し、定量RT-PCR法とウェスタンブロット法にて発現形質の変化を検討する。

また、前年度同様に蛍光光を当てた状態、またはインドシアニングリーン存在下での長期培養を行い、その細胞への影響を、細胞死、細胞接着能、細胞分裂能、細胞移動能について検討する。細胞死については、培養時にトリパンブルー法で死細胞数を測定する。接着に関しては、長期培養後に継代し、その際の接着性を見る。分裂能は、ATP法により細胞増殖能を測定し比較する。細胞移動能は、長期培養後にスクラッチを行い、そこからの移動距離で検討する。

倫理面への配慮

該当なし

C 研究結果

主に血管系の頭蓋内病変における経時的モニタリングを行う目的から、幾つかの血管作動性物質およびその受容体と動脈硬化性病変に関わると考えられている受容体や接着分子のメカニカルストレス下における発現変化について検討した。その結果、ストレックスシステムによるメカニカルストレス下での培養により血管内皮細胞および血管平滑筋細胞とも各々発現形質の変化に一定の傾向が見られた。

蛍光を当てた状態とインドシアニングリーン存在下での長期培養後の細胞への影響については、血管内皮細胞と血管平滑筋細胞ともに、細胞死、細胞接着能、細胞分裂能、細胞移動能すべてにおいて対照群との明らかな有意差はみられなかったが、同じ条件下でのばらつきも大きく、今後も検討が必要である。

D 考察

メカニカルストレス下での検討のため、培養細胞に対するメカニカルストレスの影響を加味した上で、今後は更に蛍光光とインドシアニングリーンの血管内皮細胞と血管平滑筋細胞に対する影響を、伸展培養下で検討する必要がある。

E 結論

伸展刺激下における上記薬物、蛍光光の影響はまだ不明であるが、培養条件自体が培養細胞に与える影響について一定の傾向があることがわかった。

F. 健康危険情報

なし

G 研究発表

1 論文

Matsushita N, Hirose M, Sanbe A, Kondo Y, Irie Y, Taira E.
Nicolandil improves electrical remodeling, leading to the prevention of electrically induced ventricular tachyarrhythmia in a mouse model of desmin-related cardiomyopathy.
Clinical and Experimental Pharmacology and Phisiology 41 (1):89－97, 2014.

2 学会発表

国際学会

E Taira, Y Kondo, Y Irie.
Features and distribution of gicerin expression in sensory nerve pathway of rat spinal cord.
23rd Neuropharmacology Conference 2013: The Synaptic Basis of Neurodegenerative Disorders, Nov. 2013 San Diego, USA

国内学会

入江康至、佐伯万騎男、近藤ゆき子、松下尚子、平英一
糸球体高血圧の新しい in vivo モデルとしての糸球体内皮細胞に対する周期的伸展刺激,
第87会日本薬理学会, 2014年3月 仙台

近藤ゆき子、松下尚子、入江康至、平英一
大動脈平滑筋初代培養細胞における伸展刺激と血管作動性物質刺激による発現形質変化
第87回日本薬理学会年会, 2014年3月 仙台

H 知的財産権の出願・登録状況

特記事項なし

厚生労働科学研究費補助金(医療機器開発推進研究事業)

分担研究報告書

脳内留置型微細内視鏡の開発と前臨床試験研究（H23-医療機器-指定-001）

研究分担者　弘瀬　雅教　岩手医科大学　薬学部　　教授

研究要旨

緒言:重症頭部外傷や重症くも膜下出血後の頭蓋内環境のモニタリングを持続的に行うことは、その治療において大変重要である。平成２４年度の結果を踏まえて脳内留置型微細内視鏡の改良と大動物を用いたインドシアニングリーン（ICG）の脳血管描出能の検討と評価をおこなう。

方法と結果:昨年度より改良した脳内留置型微細内視鏡を用いて、ICG を耳介静脈からの急速静注した時のミニブタの脳動脈の描出能を検討した。ミニブタ脳動脈の描出は、麻酔下に行った。麻酔下ミニブタの耳介静脈から 5 mg/ml の ICG を 1.25 ml 急速静注した時の脳動静脈描出は明らかであった。このことより、この改良型脳内留置型微細内視鏡は、現在臨床現場で使用されている量と同等の ICG 量で脳動静脈の描出が可能であることが証明された。

結論：本年度の結果から、改良した脳内留置型微細内視鏡を用いた ICG による脳動脈の描出は、臨床の場で十分対応可能なものであることが証明された。この結果を踏まえて、ICG による脳動脈描出検査のタイムテーブルや ICG による血管描出法の最適化や異常を鋭敏に検出するソフトの開発検討がおこなえる。

A. 研究目的

本研究の目的は、重症頭部外傷や重症くも膜下出血後の頭蓋内環境のモニタリングを持続的に行うための、脳内留置型微細内視鏡の開発とその前臨床試験を行うことである。本年度は、大動物を用いたインドシアニングリーン（ICG）による脳血管機能解析法開発とその基盤となる ICG の脳血管描出能を検討する。

B. 研究方法

１．新規開発した脳内留置型内視鏡の試作品を

１．改良された脳内留置型内視鏡の試作品を用いて、ICG を耳介静脈から急速投与した時のミニブタ脳動静脈の描出能の検討

a. 麻酔下ミニブタの耳介静脈より ICG を急性投与したときの脳動脈描出能を検討する。

b. 現在臨床現場で使用されている量の ICG を用いて脳動脈描出能の検討をおこない、ICG 投与による脳内留置型微細内視鏡を用いた脳動脈描出の安全性について検討する。

倫理面への配慮

動物モデル（ラット・ウサギ・ミニブタ）を用いた微細内視鏡の脳内留置実験による安全性試験とその後の組織化学的解析については、岩手医科大学動物実験験委員会において承認を受けた実験計画に基づいて行った。

C. 研究結果：

まず、麻酔下ミニブタの耳介静脈からICGを急性投与し、改良した脳内留置型内視鏡の試作品を用いて励起光を照射し蛍光を計測したところ、脳動静脈からの蛍光を検出でき、血管が描出された。次に、現在臨床の現場で使用されているICG（0.1-0.3 mg/kg)量を耳介静脈より急性投与したところ、明らかな脳動静脈の描出が認められた。

D. 考察

これまでの最近の知見によると、ICGによる脳主幹動脈の血流状態観察に用いられる一回投与量は0.1-0.3 mg/kgを急速静注することで十分な血管の描出像が得られている。今回の実験においても同等のICG量を用いて改良した脳内留置型内視鏡の試作品で脳動静脈の描出が認められた。このことより、今回試作された脳内留置型内視鏡は、大動物及び人において臨床使用量のICG投与により脳動静脈を描出することが十分可能であることが示唆される。

ICGが最大量としてどの程度使用可能かについては検討が必要であるが、文献的には脳外科手術中の最大使用可能量は一日あたり5 mg/kgとされている。術中は短時間で使用するが、外傷時や動脈瘤手術後の血管の変化を見る場合ある程度長期になり、一回投与量と１日の最大量を踏まえて、ほぼ10回／日の検査が可能であるが、どのタイミングで検査するのが最適化について、臨床の場で検査のタイムテーブル作成の検討が必要である。また将来的には肝臓・腎臓機能が低下した高齢者においても検討が必要である。

外傷時や動脈瘤手術後には、血管の機能変化である収縮・拡張の度合いを知ることが大変重要である。ICGを用いた血管の描出において早期の血管収縮・拡張（血管径の変化）を明らかにすることは大変困難である。しかし、ICGの蛍光強度の時間的変化を測定して、（時間-蛍光強度カーブの作成：半定量的な解析が可能）血流変化から間接的に血管径の変化を捉えることは可能である。今回の実験において臨床量のICGを用いて改良した脳内留置型内視鏡の試作品で脳動静脈の描出が認められたことから、ICGの蛍光強度の時間的変化を測定することにより、血管の異常を鋭敏に検出することのできるシステムの開発に繋げたい。

E. 結論

本年度の結果から、改良した脳内留置型微細内視鏡を用いたICGによる脳動脈の描出は、臨床の場で十分対応可能なものであることが証明された。このことより、臨床の場で脳内留置型微細内視鏡を用いたICGによる脳動脈描出検査のタイムテーブルとICGによる血管の機能評価について検討できる素地ができた。

F. 健康危険情報

なし

G. 研究発表

1. 論文

Misaka T, Suzuki S, Miyata M, Kobayashi A, Shishido T, Ishigami A, Saitoh S, Hirose M, Kubota I, Takeishi Y.

Deficiency of senescence marker protein 30 exacerbates angiotensin II-induced cardiac remodelling.
Cardiovasc Res 99(3):461-70, 2013.

Laurita KR, Hirose M.
Electrical vagal stimulation and cardioprotection.
Heart Rhythm 10(11):1708-1709, 2013.

Kashihara T, Hirose M, Shimojo H, Nakada T, Gomi S, Hongo M, Yamada M.
β2-Adrenergic and M2-muscarinic receptors decrease basal t-tubular L-type Ca2+ channel activity and suppress ventricular contractility in heart failure.
Eur J Pharmacol 724: 122-131, 2013.

Matsushita N, Hirose M, Sanbe A, Kondo Y, Irie Y, Taira E.
Nicorandil improves electrical remodeling, leading to the prevention of electrically induced ventricular tachyarrhythmia in a mouse model of desmin-related cardiomyopathy.
Clin Exp Pharm Physiol , 41(1): 89-97, 2014

2. 学会発表

国際学会

Hirose M, Sanbe A, Matsushita N, Taira E
Mechanisms for electrically-induced ventricular tachyarrhythmia in a mouse model of desmin-related cardiomyopathy.
The 30rd Annual Meeting of ISHR Japanese Section, San Diego USA, 2013. 6

Matsushita N, Hirose M, Takeishi Y, Shimojo H, Nakada T, Kashihara T, Mende U, Taira E, Yamada M
Transient cardiac expression of constitutively active galpha q activates renin-angiotensin system, leading to progressive heart failure and ventricular arrhythmias in transgenic mice.
American Heart Association BCVS 2013, Las Vegas USA, 2013. 7

国内学会

松下　尚子、弘瀬　雅教、平　英一
虚血誘発心臓不整脈とATP感受性K+チャネル.
第87回に本薬理学会年会　仙台, 2014, 3

H.知的財産権の出願・登録状況
特記事項なし

研究成果の刊行に関する一覧表

雑誌

発表者氏名	論文タイトル名	発表誌名	巻号	ページ	出版年
Matsushita N, Hirose M, Sanbe A, Kondo Y, Irie Y, Taira E.	Nicolandil improves electrical remodeling, leading to the prevention of electrically induced ventricular tachyarrhythmia in a mouse model of desmin-related cardiomyopathy.	Clinical and Experimental Pharmacology and Phisiology	41 (1)	89－97	2014
Nomura J, Ogasawara K, Saito H, Terasaki K, Matsumoto Y, Takahashi Y, Ogasawara Y, Saura H, Yoshida K, Sato Y, Kubo Y, Ogawa A.	Combination of blood flow asymmetry in the cerebral and cerebellar hemispheres on brain perfusion SPECT predicts 5-year outcome in patients with symptomatic unilateral major cerebral artery occlusion.	Neurological Research	36(3)269	262-269	2014
Saito H, Ogasawara K, Nishimoto H, Yoshioka Y, Murakami T, Fujiwara S, Sasaki M, Kobayashi M, Yoshida K, Kubo Y, Beppu T, Ogawa A.	Postoperative changes in cerebral metabolites associated with cognitive improvement and impairment after carotid endarterectomy: a 3T proton MR spectroscopy study.	American journal of Neuroradiology	34(5)	976-982	2013

Ohsawa M, Tanno K, Itai K, Tanvir Chowdhury Turin, Okamura T, Ogawa A, Ogasawara K, Fujioka T, Onoda T, Yoshida Y, Omama S, Ishibashi Y, Nakamura M, Makita S, Tanaka F, Kuribayashi T, Koyama T, Sakata K, Okayama A.	Comparison of predictability of future cardiovascular events between chronic kidney disease (CKD) stage based on CKD epidemiology collaboration equation and that based on modification of diet in renal disease equation in the japanese general population Iwate KENCO Study.	Circulation Journal	77(5)	1315-1325	2013
Takahashi Y, Ogasawara K, Matumoto Y, Kobayashi M, Yoshida K, Kubo Y, Beppu T, Murakami T, Nanba T, Ogawa A.	Changes in cognitive function after carotid endarterectomy in older patients: comparison with younger patients.	Neurologia medico-chirurgica	53(6)	353-359	2013

Matsumoto Y, Ogasawara K, Saito H, Terasaki K, Takahashi Y, Ogasawara Y, Kobayashi M, Yoshida K, Beppu T, Kubo Y, Fujiwara S, Tsushima E, Ogawa A.	Detection of misery perfusion in the cerebral hemisphere with chronic unilateral major cerebral artery steno-occlusive disease using crossed cerebellar hypoperfusion: comparison of brain SPECT and PET imaging.	European Journal of Nuclear Medicine and Molecular Imaging	40(10)	1573-1581	2013
Oikawa K, Ogasawara K, Saito H, Yoshida Koji, Saura H, Sato Y, Terasaki K, Wada T, Kubo Y.	Combined measurement of cerebral and cerebellar blood flow on preoperative brain perfusion SPECT imaging predicts development of new cerebral ischemic events after endarterectomy for symptomatic unilateral cervical carotid stenosis.	Clinical Nuclear Medicine	38(12)	957-961	2013

Sato Yuiko, Ito K, Ogasawara K, Sasaki M, Kudo K, Murakami T, Nanba T, Nishimoto H, Yoshida K, Kobayashi M, Kubo Y, Mase T, Ogawa A.	Postoperative increase in cerebral white matter fractional anisotropy on diffusion tensor magnetic resonance imaging is associated with cognitive improvement after uncomplicated carotid endarterectomy: tract-based spatial statistics analysis.	Neurosurgery	73(4)	592-599	2013
Misaka T, Suzuki S, Miyata M, Kobayashi A, Shishido T, Ishigami A, Saitoh S, Hirose M, Kubota I, Takeishi Y.	Deficiency of senescence marker protein 30 exacerbates angiotensin II-induced cardiac remodelling.	Cardiovasc Research	99(3)	461-70	2013
Laurita KR, Hirose M.	Electrical vagal stimulation and cardioprotection.	Heart Rhythm	10(11)	1708-1709	2013
Kashihara T, Hirose M, Shimojo H, Nakada T, Gomi S, Hongo M, Yamada M.	β2-Adrenergic and M2-muscarinic receptors decrease basal t-tubular L-type Ca2+ channel activity and suppress ventricular contractility in heart failure.	European Journal of Pharmacology	724	22-131	2013

Clinical and Experimental Pharmacology and Physiology (2014) **41**, 89–97 doi: 10.1111/1440-1681.12185

Nicorandil improves electrical remodelling, leading to the prevention of electrically induced ventricular tachyarrhythmia in a mouse model of desmin-related cardiomyopathy

Naoko Matsushita,*† Masamichi Hirose,* Atsushi Sanbe,‡ Yukiko Kondo,† Yasuyuki Irie† and Eiichi Taira†

**Department of Molecular and Cellular Pharmacology, Iwate Medical University School of Pharmaceutical Sciences, †Department of Pharmacology, Iwate Medical University School of Medicine, and ‡Department of Pharmacotherapeutics, Iwate Medical University School of Pharmaceutical Sciences, Shiwa-gun, Iwate, Japan*

SUMMARY

1. Transgenic (TG) mice overexpressing an arg120gly missense mutation in heat shock protein B5 (*HSPB5*; i.e. R120G TG mice) exhibit desmin-related cardiomyopathy. Recently, the cardioprotective effect of nicorandil has been shown to prolong the survival of R120G TG mice. However, whether the TG mice exhibit ventricular arrhythmias and whether nicorandil can inhibit these arrhythmias remain unknown. In the present study we examined the effects of chronic nicorandil administration on ventricular electrical remodelling and arrhythmias in R120G TG mice.

2. Mice were administered nicorandil (15 mg/kg per day) or vehicle (water) orally from 5 to 30 weeks of age. Electrocardiograms (ECG) and optical action potentials were recorded from R120G TG mouse hearts. In addition, the expression of ventricular connexin 43 and the cardiac Na^+ channel Nav1.5 was examined in TG mice.

3. All ECG parameters tested were prolonged in R120G TG compared with non-transgenic (NTG) mice. Nicorandil improved the prolonged P, PQ and QRS intervals in R120G TG mice. Interestingly, impulse conduction slowing and increases in the expression of total and phosphorylated connexin 43 and Nav1.5 were observed in ventricles from R120G TG compared with NTG mice. Nicorandil improved ventricular impulse conduction slowing and normalized the increased protein expression levels of total and phosphorylated connexin 43, but not of Nav1.5, in R120G TG mouse hearts. Electrical rapid pacing at the ventricle induced ventricular tachyarrhythmias (VT) in six of eight R120G TG mouse hearts, but not in any of the eight nicorandil-treated R120G TG mouse hearts ($P < 0.05$).

4. These findings demonstrate that nicorandil inhibits cardiac electrical remodelling and that the prevention of VT by nicorandil is associated with normalization of connexin 43 expression in this model.

Key words: connexin 43, desmin-related cardiomyopathy, heat shock protein B5, Nav1.5, nicorandil, ventricular tachyarrhythmia.

INTRODUCTION

The anti-anginal agent nicorandil is known as an opener of the ATP-sensitive potassium (K_{ATP}) channel and has a nitrate moiety.[1] Considerable clinical evidence has demonstrated that nicorandil protects the heart against ischaemic injury,[1] improves the recovery of postischaemic contractile dysfunction and can reduce infarct size in several animal models.[2] The Impact Of Nicorandil In Angina (IONA) study, a randomized placebo-controlled study, has shown that nicorandil reduces the incidence of major cardiovascular events in patients with angina pectoris.[1,3] Moreover, recent studies suggest that the cardioprotective effects of nicorandil are mediated by activation of mitochondrial (mito) K_{ATP} channels in myocytes.[2,4]

Desmin mutations in humans cause desmin-related cardiomyopathy, resulting in heart failure, atrial and ventricular arrhythmias and sudden cardiac death. Desmin appears to play a critical role in maintaining the structural integrity of muscle cells and transmitting force generated by contraction by forming a continuous network of filaments that link desmosomes at cell-to-cell adhesion complexes to intracellular components of the contractile apparatus.[5] The R120G missense mutation in heat shock protein B5 (*HSPB5*) can cause desmin-related cardiomyopathy.[6] This disease is a misfolded protein-related disease that can be recapitulated in transgenic (TG) mice by expressing the mutant HSPB5 R120G protein (R120G TG mice) specifically in cardiomyocytes.[7] Hearts from R120G TG mice exhibit perinuclear aggresome formation.[8] In a previous study, we demonstrated that cell viability was dose-dependently recovered in myocytes overexpressing mutant HSPB5 (i.e. R120G TG) following treatment with nicorandil, an opener of K_{ATP} channels and nitric oxide (NO) donor.[9] Nicorandil also inhibited the increase in Bcl-2-associated X (BAX) protein, the decrease in B-cell lymphoma 2 (BCL2), activation of caspase 3 and apoptotic cell death induced by the mutant *HSPB5*.[9] Moreover, nicorandil prolonged the survival of R120G TG mice. On the basis

Correspondence: Dr Masamichi Hirose, Department of Molecular and Cellular Pharmacology, Iwate Medical University School of Pharmaceutical Sciences, Iwate 028-8621, Japan. Email: mhirose@iwate-med.ac.jp

Received 18 July 2013; revision 26 September 2013; accepted 30 September 2013.

of these results, we concluded that nicorandil prolonged the survival of R120G TG mice by protecting against mitochondrial impairments.[9] Another study demonstrated the remodelling of gap junctions and slow impulse conduction in a TG mouse model of human desmin-related cardiomyopathy with cardiac-specific expression of a seven amino acid deletion mutation in desmin.[10] However, whether R120G TG mice exhibit cardiac electrical remodelling and whether nicorandil improves the electrical remodelling in these mice remain unknown. In a previous study we demonstrated that nicorandil prevents ventricular tachyarrhythmia induction by improving ventricular electrical remodelling in a mouse model of chronic heart failure.[11] Therefore, we hypothesized that nicorandil improves cardiac electrical remodelling in R120G mice. In the present study, we examined the effects of chronic nicorandil treatment on ventricular electrical remodelling and ventricular tachyarrhythmia (VT) in R120G TG mice.

METHODS

The study protocol was approved by the institutional Animal Experiments Committee of Iwate Medical University and complied with the *Guide for Care and Use of Laboratory Animals* published by the US National Institutes of Health (NIH publication 85-23, revised 1996; http://grants.nih.gov/grants/olaw/).

Experimental animals

Mice with cardiac-specific overexpression of mutant HSPB5 containing the R120G mutation, driven by the α-myosin heavy chain promoter, have been described previously.[8] The TG mice were identified by polymerase chain reaction (PCR) analysis of genomic DNA isolated from the tail tips. Non-transgenic (NTG) littermates were always used as controls for comparison. To examine the effects of chronic nicorandil administration on ventricular electrical remodelling and the induction of arrhythmia, R120G TG mice were given nicorandil (15 mg/kg per day; kindly provided by Chugai Pharmaceutical, Tokyo, Japan) or vehicle (water) orally from 5 to 30 weeks of age. All experiments were performed in 30-week-old mice.

Immunohistochemistry

Immunohistochemical analyses were performed as described previously.[8,9,12] Alexa488-conjugated anti-rabbit and Alexa568-conjugated anti-mouse antibodies were purchased from Molecular Probes (Eugene, OR, USA), anti-connexin 43 (Cx43) antibody was from Invitrogen (Camarillo, CA, USA), anti-phosphorylated (p)-Cx43 (Ser^{368}) antibody was from Cell Signaling Technology (Danvers, MA, USA) and the anti-β-catenin antibody was from Santa Cruz Biotechnology (Santa Cruz, CA, USA).

Western blotting

Sample preparation for western blotting analysis, gel preparation and electrophoresis were performed as described previously.[8,9,12] Western blot analyses were performed using an anti-GAPDH antibody (Chemicon International, Temecula, CA, USA), an anti-Cx43 antibody (Invitrogen, Camarillo, CA, USA), an anti-p-Cx43 (Ser^{368}) antibody (Cell Signaling Technology) and an anti-Nav1.5 antibody (Aviva Systems Biology, San Diego, CA, USA). Band intensity in the immunoblots was semiquantified using ImageJ software (http://rsbweb.nih.gov/ij/), as described previously.[8,12]

Echocardiography

Mice were anaesthetized with 2% isoflurane and their cardiac function was assessed by echocardiography (Hitachi Aloka Medical, Tokyo, Japan), as described previously.[11] Hearts were viewed at the level of the papillary muscles along the short axis. In M-mode tracings, the average of three consecutive beats was used to measure left ventricular fractional shortening (LVFS).

Electrocardiography

Mice were anaesthetized with 2% isoflurane. Electrocardiogram (ECG) lead II was recorded and filtered (0.1–300 Hz), digitized with 12-bit precision at a sampling rate of 1000 Hz per channel (Microstar Laboratories, Bellevue, WA, USA) and transmitted to a microcomputer before being saved to a CD-ROM.

Langendorff-perfused mouse heart

After being anaesthetized with 2% isoflurane, mice were treated with 3.8 mg/kg, i.v., sodium heparin and hearts were quickly excised and connected to a modified Langendorff apparatus. A polytetrafluoroethylene-coated silver bipolar electrode was used to stimulate the epicardial surface of the anterior left ventricle. A monophasic action potential electrode was placed on the epicardial surface of the posterior left ventricle to record ventricular action potentials. Each preparation was perfused under constant flow conditions with oxygenated (95% oxygen, 5% CO_2) Tyrode's solution (composition (in mmol/L): NaCl 141.0; KCl 5.0; $CaCl_2$ 1.8; $NaHCO_3$ 25.0; $MgSO_4$ 1.0; NaH_2PO_4 1.2; HEPES 5; dextrose 5.0, pH 7.4 at 36 ± 1°C). Perfusion pressure was measured with a pressure transducer (Nihon Kohden, Tokyo, Japan) and maintained within the pressure range 50–60 mmHg by adjusting flow. Preparations were stained with 5 μL voltage-sensitive dye (di-4-ANEPPS; Molecular Probes), dissolved in 0.19 mL ethanol to a concentration of 8 μmol/L. Cardiac rhythm was monitored using three silver disk electrodes fixed to the chamber in positions corresponding to ECG limb leads II.

Optical mapping system

In every experiment, the mapping field was positioned at the anterior left ventricle, including a part of the right ventricle. The optical mapping system used in the present study has been described in detail elsewhere.[13] Briefly, signals recorded from each photodiode and ECG signals were multiplexed and digitized with 12-bit precision at a sampling rate of 3000 Hz per channel (Microstar Laboratories). An optical magnification of ×3 was used, corresponding to a mapping field of 0.6 × 0.6 cm and 0.37 mm spatial resolution between recording pixels.

Experimental protocol

Age-matched NTG, R120G TG and R120G TG + nicorandil-treated (R120G TG + Nico) mice ($n = 8$ in each group) were used. First, ECG lead II was recorded for 10 min in all mice. Second, to measure action potential duration (APD) and conduction velocity (CV), monophasic and optical action potentials were recorded for 10 s from the epicardial surface of the posterior and anterior left ventricles at basic cycle lengths of 200, 150 and 100 msec in isolated hearts. Third, rapid ventricular pacing at a pacing cycle length of 80–100 msec for approximately 5 s from the surface of the anterior left ventricle was performed to induce VT. In the present study, VT was defined as a rapid (cycle length < 100 msec) regular or irregular rhythm persisting for more than 10 beats. Ventricular rapid pacing was performed 10 times to induce VT. Optical action potentials were recorded during the VT from the epicardial surface of the anterior left ventricle for 10 s.

Data analysis

In all anaesthetized mice, P, PR and QRS complex, QT, QTc and RR intervals were measured from ECG lead II. In all monophasic and optical action potentials recorded from Langendorff hearts, depolarization time was defined as the point of the maximum positive derivative in the action potential upstroke (dV/dt_{max}). Depolarization contour maps were computed for the entire mapping field. Repolarization time was defined as the time when repolarization reached a level of 90%. The monophasic APD_{90} was defined as the difference between repolarization time and depolarization time. Mean monophasic APD_{90} was calculated from the average of monophasic APD_{90} from more than three consecutive beats. The upstroke ratio of Phase 0 depolarization was calculated as the ratio of the width of *a* to that of *b* from monophasic and optical action potential. The method of Bayly *et al.*[14] was modified for optically recorded action potential maps for accurate quantification of the direction and magnitude of CV at each recording site. Mean CV was calculated from the average of local CV at more than 100 sites.

All data are given as the mean±SEM. Analysis of variance with Bonferroni's test was used for the analysis of multiple comparisons of data. Fisher's exact test was used to compare the incidence of VT between different conditions. $P < 0.05$ was considered significant.

RESULTS

Cardiac contractile function and heart weight : bodyweight ratio

In the present study, M-mode echocardiograms demonstrated that, compared with NTG mice, R120G TG mice exhibited impaired left ventricular contractility, as demonstrated by the marked reduction in LVFS (Fig. 1a), which is consistent with previous results from TG mice.[8] Nicorandil significantly improved the reduced LVFS in R120G TG mice (Fig. 1a). The heart weight : bodyweight ratio was increased in R120G TG compared with NTG mice, and nicorandil treatment significantly reduced this ratio in R120G TG mice (Table 1).

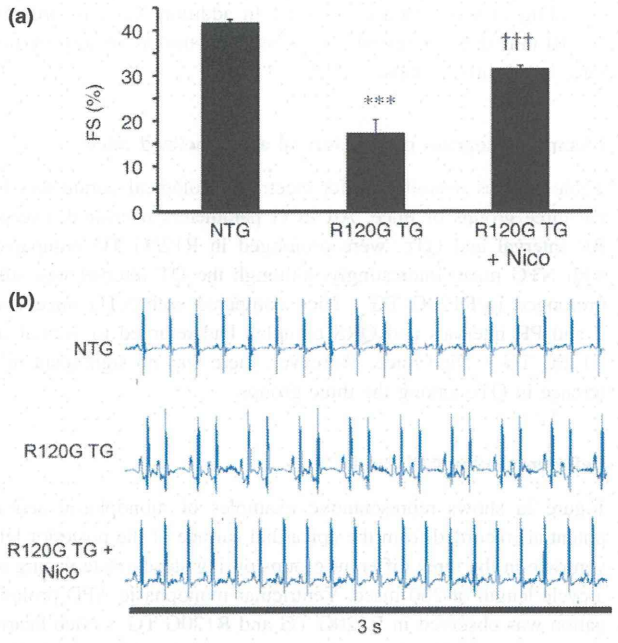

Fig. 1 (a) Left ventricular fractional shortening (FS) in non-transgenic (NTG) mice, mice overexpressing an arg120gly missense mutation in heat shock protein B5 (*HSPB5*; i.e. R120G TG mice) and nicorandil-treated (+ Nico) R120G TG mice. Data are the mean±SEM ($n = 8$ in each group). (b) Representative electrocardiogram lead II recordings from each of the three groups of mice.

Table 1 General parameters and the incidence of ventricular tachyarrhythmia in the three groups

	NTG	R120G TG	R120G TG + Nico
Body weight (g)	31.2 ± 2.5	33.7 ± 1.0	32.8 ± 0.7
Heart weight (mg)	167 ± 5	296 ± 13***	188 ± 15†††
Heart weight : body weight (mg/g)	5.6 ± 0.6	8.8 ± 4.0***	5.7 ± 0.3††
VT induction (Langendorff heart)	0/8	6/8*	0/8†

Data are the mean±SEM ($n = 8$ mice in each group). *$P < 0.05$, ***$P < 0.001$ compared with non-transgenic mice (NTG); $^{\dagger}P < 0.05$, $^{\dagger\dagger}P < 0.01$, $^{\dagger\dagger\dagger}P < 0.001$ compared with mice overexpressing an arg120-gly missense mutation in heat shock protein B5 (*HSPB5*; i.e. R120G TG mice).

VT, ventricular tachyarrhythmia; R120G TG + Nico, nicorandil-treated R120G TG mice.

Arrhythmia induction in anaesthetized mice

Figure 1b shows representative ECG recordings from three different groups (NTG, R120G TG, R120G TG + Nico mice) and sinoatrial block or the failure of sinus node function in an R120G TG mouse can be clearly seen. Such sinoatrial block was observed in two of eight R120G TG mice. In contrast, two ECG recordings from NTG and R120G TG + Nico mice showed a P wave and QRS complex with a regular RR interval without any arrhythmia, indicating sinus rhythm. All NTG and R120G TG + Nico mice tested showed sinus rhythm during ECG

recording over a period of 10 min. In addition, ECG recordings for 10 min did not reveal any other arrhythmias in any of the mice in all three groups.

Electrocardiogram parameters in anaesthetized mice

Table 2 gives overall data for electrophysiological parameters in the three groups of mice. All ECG parameters measured, except RR interval and QTc, were prolonged in R120G TG compared with NTG mice. Interestingly, although the QT interval was still prolonged in R120G TG + Nico compared with NTG mice, the P and PR intervals and QRS complex had returned to normal in R120G TG + Nico mice. Moreover, there was no significant difference in QTc among the three groups.

Left ventricular APD and CV

Figure 2a shows representative examples of monophasic action potentials recorded from the epicardial surface of the posterior left ventricle in the three different groups during steady state pacing at a cycle length of 200 msec. Ventricular monophasic APD prolongation was observed in R120G TG and R120G TG + Nico hearts compared with NTG hearts. Mean monophasic APD was significantly prolonged in left ventricles from R120G TG and R120G TG + Nico mice compared with NTG mice at pacing cycle lengths of 200 and 150 msec (Fig. 2b). Interestingly, levels of mean monophasic APD were similar among the three groups at a pacing cycle length of 100 msec. Figure 3a shows representative examples of activation isochrone maps recorded from the epicardial surface of the anterior left ventricle during steady state pacing at cycle lengths of 200, 150 and 100 msec in the three groups. Relative crowding of isochrone lines for R120G TG hearts (Fig. 3b) indicates conduction slowing compared with NTG and R120G TG + Nico hearts (Fig. 3b). In addition, when considering all experiments (Fig. 3b), the mean CV of the left ventricle was significantly slower in R120G TG than NTG hearts, and nicorandil significantly improved the decreased CV in R120G TG hearts.

Induction of VT in Langendorff-perfused heart

Before rapid pacing, spontaneous VT was not observed in any Langendorff-perfused NTG, R120G TG and R120G TG + Nico hearts. Rapid pacing induced VT in six of eight R120G hearts (Table 1). In contrast, rapid pacing did not induce VT in any NTG and R120G TG + Nico hearts (Table 1). Nicorandil significantly reduced the incidence of VT induction by rapid pacing in R120G TG hearts ($P < 0.05$). Figure 4 shows an example of electrically induced VT in a Langendorff-perfused R120G TG heart. A representative ECG and monophasic action potential signal during VT showed rapid repetitive activation at a cycle length of <50 msec without pacing.

Table 2 Electrocardiographic parameters in the three groups

Parameters (msec)	NTG	R120G TG	R120G TG + Nico
P	20 ± 1	34 ± 2***	25 ± 2††
RR	201 ± 20	235 ± 40	203 ± 21
PR	45 ± 5	62 ± 8**	47 ± 8†
QRS	16 ± 1	20 ± 1**	17 ± 1†
QT	34 ± 1	39 ± 2**	37 ± 1*
QTc	77 ± 3	84 ± 4	83 ± 2

Data are the mean±SEM ($n = 8$ mice in each group). *$P < 0.05$, **$P < 0.01$, ***$P < 0.001$ compared with non-transgenic mice (NTG); †$P < 0.05$, ††$P < 0.01$compared with mice overexpressing an arg120gly missense mutation in heat shock protein B5 (*HSPB5*; i.e. R120G TG mice).

R120G TG + Nico, nicorandil-treated R120G TG mice.

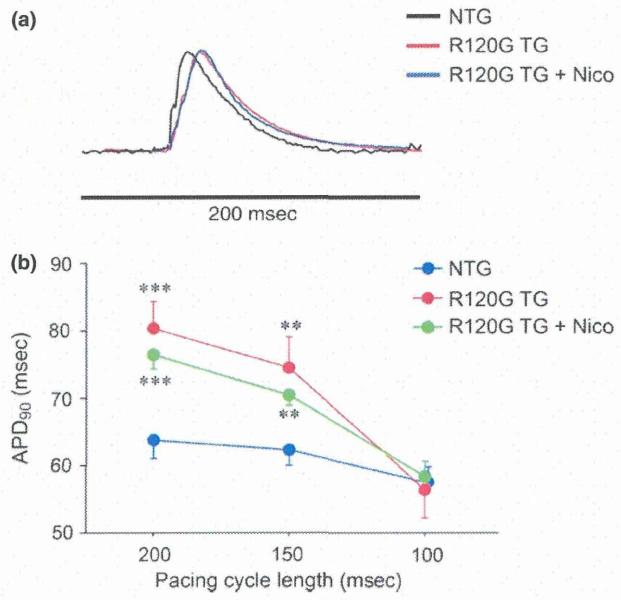

Fig. 2 Monophasic action potential duration (APD) recorded from the epicardial surface of the posterior left ventricle in non-transgenic (NTG) mice, mice overexpressing an arg120gly missense mutation in heat shock protein B5 (*HSPB5*; i.e. R120G TG mice) and nicorandil-treated (+ Nico) R120G TG mice. (a) Representative traces showing monophasic action potentials recorded from the epicardial surface of the posterior left ventricle in the three groups during steady state pacing at a cycle length of 200 msec. (b) Mean monophasic APD_{90} calculated from the average of APD_{90} from more than three consecutive beats. Mean monophasic APD_{90} was significantly prolonged in ventricles from R120G TG compared with NTG mice. Data are the mean±SEM ($n = 8$ in each group). **$P < 0.01$, ***$P < 0.001$ compared with the NTG group.

Connexin 43 expression and spatial distribution pattern

Figure 5a shows the immunolocalization of total Cx43 proteins in the left ventricle from NTG, R120G TG and R120G TG + Nico mice. As can be seen from the immunolabelling distribution patterns of total Cx43 protein, the expression of Cx43 protein was upregulated and linear staining of Cx43 at the lateral cell margins greatly increased in R120G TG compared with NTG hearts. Moreover, Cx43 was heterogeneously stained at intercalated discs of R120G TG compared with NTG mouse ventricles. Interestingly, nicorandil treatment decreased the linear staining of Cx43 at the lateral cell margins in R120G TG hearts. Figure 5c shows Cx43 expression in each group, demonstrating that the anti-Cx43 antibody identified the Cx43 protein and overall expression in left ventricles from mice in each group. The

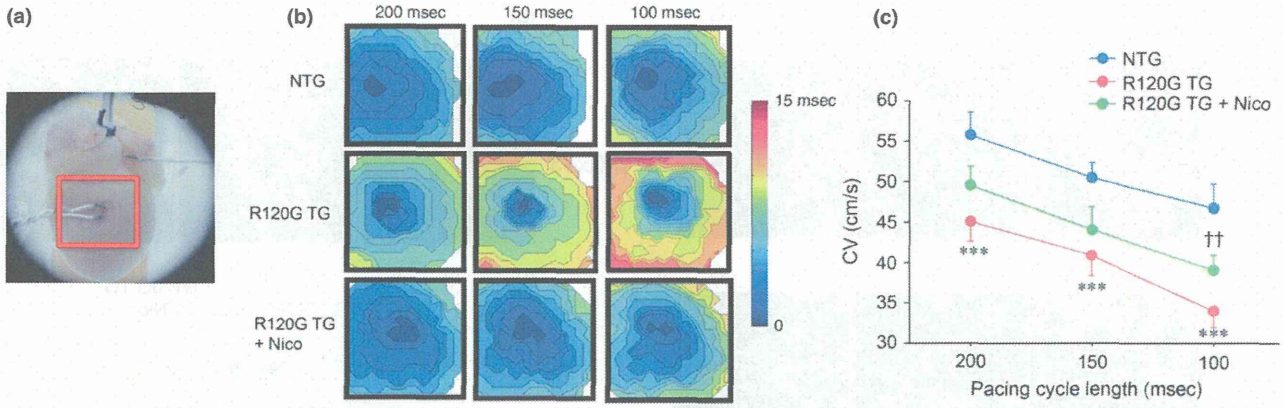

Fig. 3 Impulse conduction velocity (CV) recorded from the epicardial surface of the anterior left ventricle in non-transgenic (NTG) mice, mice overexpressing an arg120gly missense mutation in heat shock protein B5 (*HSPB5*; i.e. R120G TG mice) and nicorandil-treated (+ Nico) R120G TG mice. (a) Photograph of the mapping area (red box) showing the pacing electrode and the anterior left ventricle including part of the right ventricle. (b) Representative activation isochrone maps from each of the three groups during steady state pacing at cycle lengths of 200, 150 and 100 msec. Activation maps are shown with 1 msec isochrones. (c) Mean CV calculated from the local CV at more than 100 sites. Data are the mean±SEM (n = 8 in each group). ***$P < 0.001$ compared with the NTG group; $^{\dagger\dagger}P < 0.01$ compared with the R120G TG group.

relative expression of total Cx43 protein was significantly greater in R120G TG than NTG ventricles and nicorandil significantly decreased Cx43 expression to normal levels in R120G TG ventricles (Fig. 5c). Figure 5b shows the immunolocalization of p-Cx43 proteins in left ventricles from NTG, R120G TG and R120G TG + Nico mice. The expression of Cx43 protein was upregulated in R120G TG compared with NTG hearts. Nicorandil treatment decreased the expression of p-Cx43 in R120G TG ventricles (Fig. 5b). Figure 5d,e shows expression levels of p-Cx43 proteins in left ventricular tissue from the three different groups. Similar to total Cx43, the expression of p-Cx43 protein was increased in R120G TG ventricles and nicorandil inhibited this increase in p-Cx43 expression. To determine changes in p-Cx43 and total Cx43 expression, the ratio of p-Cx43 : total Cx43 was calculated (Fig. 5f). There were no significant differences in this ratio among the three different groups.

Upstroke ratio of Phase 0 depolarization and Nav1.5 expression

The upstroke velocity of Phase 0 depolarization depends on Na^+ channel activity and plays an important role in the impulse conduction. Therefore, we examined changes in the upstroke velocity of Phase 0 depolarization using the upstroke ratio of Phase 0 depolarization from monophasic action potentials (Fig. 6a) and the protein expression of Nav1.5 in R120G TG mouse hearts. Figure 6b shows the upstroke ratio of Phase 0 depolarization in the left ventricle in each of the three groups. The upstroke ratio calculated from the monophasic action potential was significantly lower in ventricles from R120G TG than NTG mice, and nicorandil did not improve it (Fig. 6b). In contrast, although the upstroke ratio of Phase 0 depolarization calculated from the optical action potential was significantly lower in ventricles from R120G TG than NTG mice, it was improved by nicorandil treatment (Fig. 6c). Figure 6d,e shows the expression of Nav1.5 proteins in left ventricular tissue from the three different groups. Figure 6d shows a representative example of protein expression in each group and demonstrates that the anti-Nav1.5 antibody

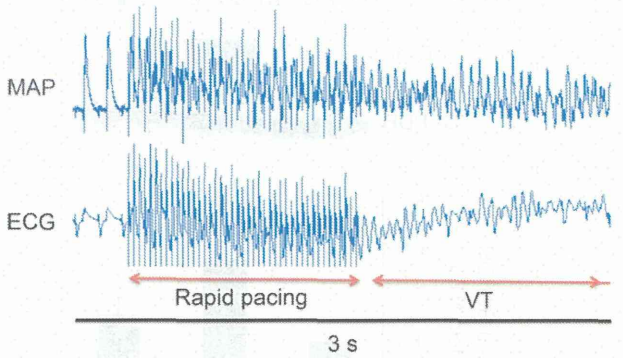

Fig. 4 Example of electrically induced ventricular tachyarrhythmia (VT) in a Langendorff-perfused heart from a mouse overexpressing an arg120-gly missense mutation in heat shock protein B5 (*HSPB5*; i.e. R120G TG group). MAP, monophasic action potential; ECG, electrocardiogram.

identified the Nav1.5 protein. The relative expression levels of Nav1.5 proteins were significantly greater in ventricles from R120G TG than NTG mice, and nicorandil did not improve them in (Fig. 6e).

DISCUSSION

Mean monophasic APD was significantly prolonged in ventricles from R120G TG than NTG mice. Moreover, mean CV for the left ventricle was significantly slower in R120G TG than NTG mice. It is well known that re-entry can induce VT. Re-entry requires a suitable vulnerable substrate. Ventricular remodelling has the potential to increase the likelihood of re-entrant activity through a suitable vulnerable substrate. For example, electrophysiological remodelling, such as refractory period shortening (i.e. APD shortening) and slowing of impulse conduction, can promote re-entry. Re-entry was first defined by Mines in 1914 as a persisting electrical impulse that reactivates an area of previously activated myocardial tissue that is no longer refractory, resulting in a circular movement of activation.[15] The length of such a

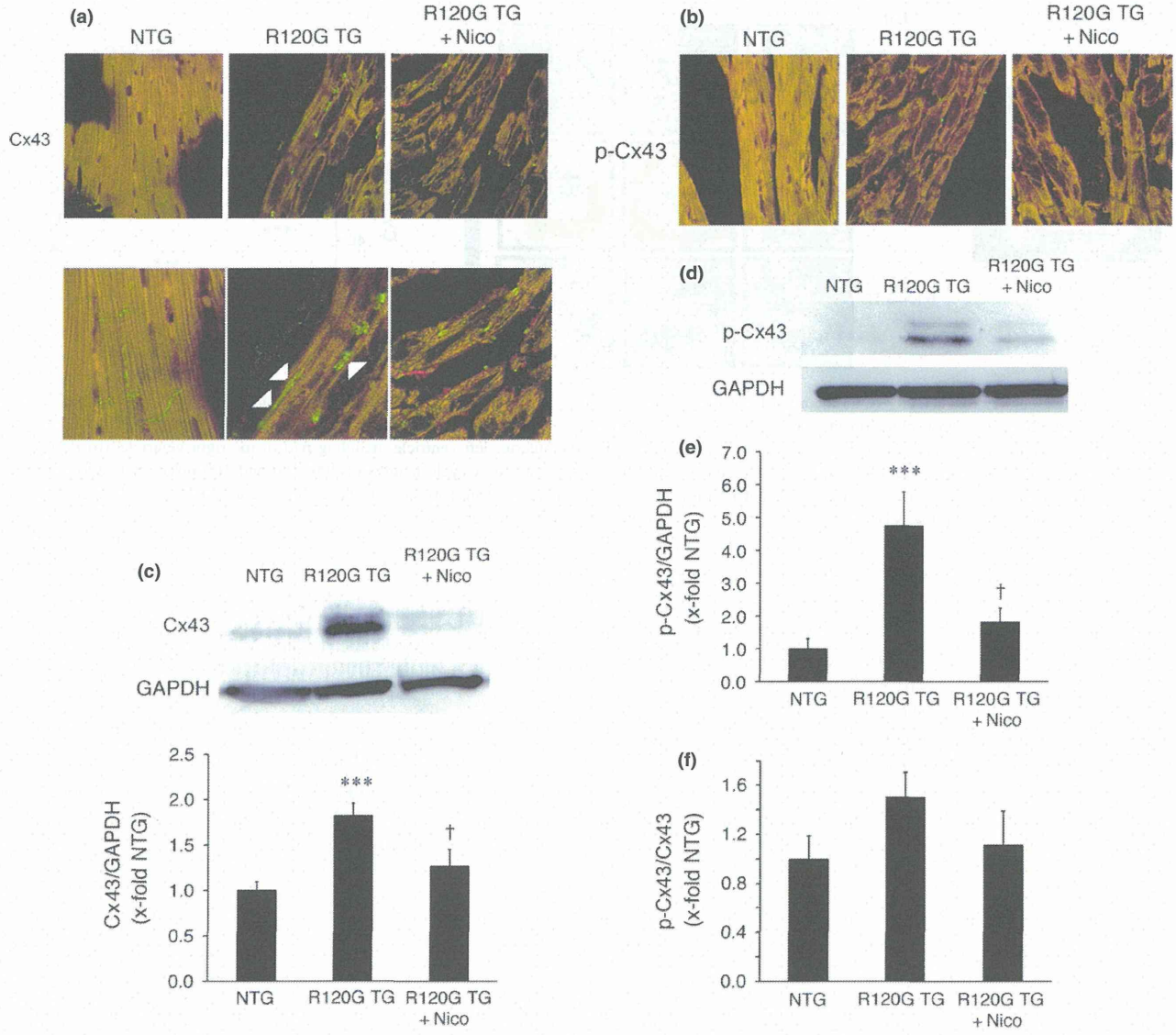

Fig. 5 (a,b) Immunofluorescent confocal images stained for β-catenin (red) and (a) total and (b) phosphorylated (p-) connexin43 (Cx43; green). Longitudinal sections are shown for samples from non-transgenic (NTG) mice, mice overexpressing an arg120gly missense mutation in heat shock protein B5 (*HSPB5*; i.e. R120G TG mice) and nicorandil-treated (+ Nico) R120G TG mice. Arrowheads indicate examples of lateralized staining. (c) Representative immunoblots and summary of results of total Cx43 expression in samples of ventricular tissue from NTG, R120G TG and R120G TG + Nico mice. (d,e) Representative immunoblots (d) and summary of results (e) of p-Cx43 expression in samples from NTG, R120G TG and R120G TG + Nico mice. (f) Ratio of p-Cx43 : total Cx43 protein expression in each of the three groups. In all cases, Cx43 expression was normalized against that of GAPDH expression and is expressed relative to that in the NTG group (set at 1). Data are the mean±SEM from six mice in each group. $^{***}P < 0.001$ compared with the NTG group; $^{\dagger}P < 0.05$ compared with the R120G TG group.

cycle depends on its wavelength, defined by the mathematical product of the refractory period and the CV (plus an excitable gap when present). In the present study, mean monophasic APD was significantly prolonged in ventricles from R120G TG than NTG mice at longer pacing cycle lengths (200 and 150 msec), whereas at a shorter pacing cycle length (100 msec) mean monophasic APD was shorter in ventricles from R120G TG mice, similar to that in the NTG group. Moreover, mean CV for the left ventricle was significantly slower in R120G TG than in NTG mice, suggesting that the electrical remodelling, especially CV slowing, favours the induction of re-entrant activation because of shortening of the wavelength. In fact, electrically induced VT caused re-entry in the present study (see Movie S1, available as Supplementary Material to this paper). Nicorandil did not improve the prolongation of monophasic APD in left ventricles from R120G TG compared with NTG mice, regardless of pacing cycle length, whereas it inhibited decreases in CV in ventricles from R120G TG mice. These results suggest that nicorandil can increase the wavelength of the re-entrant circuit, leading to inhibition of VT. In fact, electrically induced VT was not induced in any of the eight ventricles from nicorandil-treated R120G TG mice in the present study.